Mode selective chemistry in the reactions of OH with HBr and HCl

David C. Clary, Gunnar Nyman, and Ramon Hernandez

Citation: The Journal of Chemical Physics **101**, 3704 (1994); doi: 10.1063/1.468467
View online: http://dx.doi.org/10.1063/1.468467
View Table of Contents: http://scitation.aip.org/content/aip/journal/jcp/101/5?ver=pdfcov
Published by the AIP Publishing

Mode selective chemistry in the reactions of OH with HBr and HCl

David C. Clary, Gunnar Nyman, and Ramon Hernandez
Department of Chemistry, University of Cambridge, Lensfield Road, Cambridge CB2 1EW, United Kingdom

(Received 17 March 1994; accepted 10 May 1994)

Quantum scattering calculations are reported for the reactions $OH+HCl \rightarrow H_2O+Cl$ and $OH+HBr \rightarrow H_2O+Br$. The rotating bond approximation is used. This involves the explicit treatment of the bending vibration and local OH stretching vibration in H_2O together with the vibration of HX (X=Cl,Br) and rotation of OH. Simple potential energy surfaces for the reactions are used which contain an accurate potential for H_2O. The transition state of the potential for the OH+HCl reaction agrees quite well with *ab initio* data. The most likely product vibrational state of H_2O is the ground state for the $OH(j=0)+HCl$ reaction, and the combination band that has one quantum of energy in the H_2O bending mode and one quantum in the local OH stretching mode of H_2O for the $OH(j=0)+HBr$ reaction. The reaction cross sections are found to depend on $(2j+1)^{-1}$, where j is the initial rotational quantum number of OH. This results in a $T^{-1/2}$ dependence in the rate constant for the OH+HBr reaction at low temperatures, in agreement with experiment.

I. INTRODUCTION

There has been considerable recent experimental interest in the effect of exciting selected modes or bonds of polyatomic molecules taking part in chemical reactions.[1,2] Furthermore, there have been several observations on the particular vibrational states that are formed in the polyatomic products of chemical reactions.[3] The reaction between H atoms and H_2O has become a prototypical system in this regard, both from the point of view of experiment[1,2] and theory,[4–11] and strong bond and mode-selective effects have been observed in this reaction. It is of interest, therefore, to see if these effects also occur in other reactions involving H_2O as reactant or product.

In this paper, we report a theoretical study on the exothermic reactions

$$OH+HCl \rightarrow H_2O+Cl \quad (I)$$

and

$$OH+HBr \rightarrow H_2O+Br \quad (II)$$

for thermal collision energies. These reactions are very important in atmospheric chemistry as they produce Cl and Br atoms that destroy ozone.[12] The experimentally measured rate constant for the OH+HBr reaction is very large[13] and has a marked negative temperature dependence for temperatures less than 100 K.[14] This temperature dependence has not yet been explained theoretically. The experimental rate constant for the OH+HCl reaction is also quite unusual,[15] being almost independent of temperature for temperatures less than 300 K.

These two reactions are also of considerable interest because they are hydrogen atom transfer reactions of the heavy–light–heavy type. Heavy–light–heavy reactions have been studied extensively for atom+diatomic molecule systems and simple rules have emerged[16] for predicting which vibrational states are most likely to be populated during the reaction. Examinations of avoided crossings between vibrationally adiabatic potentials in hyperspherical coordinates have been particularly useful in explaining strong propensities in the vibrationally state-selected reaction probabilities of atom+diatom reactions.[16] Here, we examine whether the same ideas can be extended to heavy–light–heavy reactions involving four atoms and concentrate our study on an examination of the particular vibrational product states of H_2O that are formed and on the effect of the initial rotational states of OH on the reaction.

The method we use in our calculations is the rotating bond approximation (RBA).[5] This is a three-dimensional quantum mechanical theory that, in the form applied here, accounts explicitly for the quantum numbers j, v, m, and n in a four-atom reaction

$$OH(j)+HX(v) \rightarrow H_2O(m,n)+X,$$

where j and v are the rotational and vibrational states of OH and HX, respectively, while m and n are the bending mode and a local OH stretching mode of H_2O. The rotations of HX are accounted for by applying an adiabatic bend correction. The RBA has been used in extensive calculations on the $H+H_2O \rightarrow OH+H_2$ reaction, and its isotopes, and has given comparisons with experimental results of rate constants,[5] vibrationally selected cross sections,[6,7] product rotational distributions,[10] and differential cross sections[10] for this reaction. The method has been shown to be quite accurate in calculating vibrationally selected reaction probabilities by comparison with results obtained from an exact quantum mechanical treatment of this reaction in which the four-atom geometry is constrained to a plane.[9] Furthermore, provided an adiabatic bend correction is applied, the method gives cumulative reaction probabilities for the $OH+H_2 \rightarrow H+H_2O$ reaction that agree well[17] with exact results.[18] The RBA has also been applied to the $OH+CO \rightarrow CO_2+H$ reaction[19] and the calculations have been compared in detail with classical trajectory and experimental results.

The Cl+HOD reaction has been the subject of a model quasiclassical trajectory calculation[20] in which the potential energy surface for the $H+H_2O$ reaction was used. In the present paper, a potential surface is constructed explicitly for the $OH+HCl \rightarrow H_2O+Cl$ reaction and its reverse reaction.

 0021-9606/94/101(5)/3704/11/$6.00

We report RBA calculations with this form of potential elsewhere for the Cl+HOD and Cl+H_2O reactions at higher collision energies.[21]

The potential surfaces used in our computations are of a common, flexible form for both OH+HCl and OH+HBr. A particular feature of the potentials is that they contain a very accurate potential energy surface[22] for H_2O, and the diatomic vibrations of OH and HX are also treated accurately. Consequently, the exothermicities of the reactions are correct. For OH+HCl, the transition state geometry of the potential agrees quite well with that determined from *ab initio* calculations. These simple potential energy surfaces are not expected to be of quantitative accuracy, but they are useful in enabling us to make some qualitative predictions about the rovibrational mode selectivity in these reactions.

The OH+HBr reaction is also of particular interest as it represents a neutral fast reaction with no apparent activation energy.[23] Capture theory has been applied to estimate the rate constant for this reaction[24] which is dominated at very long range by a dipole–dipole interaction. This theory does not involve a treatment of the reaction dynamics all the way from reactants to products and assumes that the reaction probability is unity for all values of the total angular momentum which give a classically allowed reaction.[25] This method gives an upper bound to the rate constant at very low temperatures, but is not expected to give accurate results for higher temperatures.

This paper is organized as follows: Section II briefly describes the rotating bond approximation and its application to the OH+HCl and OH+HBr reactions. Section III presents the potential energy surfaces used in the computations. Numerical details of the calculations are described in Sec. IV, together with some rate constant calculations that were used to test the quality of the potential energy surfaces. Section V describes calculations of vibrationally selected cross sections for the OH+HCl and OH+HBr reactions and also presents a rationalization of the results in terms of avoided crossings of rovibrationally adiabatic potentials obtained in hyperspherical coordinates. The rate constants for these reactions are also calculated and a new explanation for the unusual temperature effects observed in these reactions is also deduced from the theoretical results. Conclusions are in Sec. VI.

II. ROTATING BOND APPROXIMATION

A. Coordinates and Hamiltonians

We present a brief description of the rotating bond approximation applied to the $OH(j)+HX(v)\rightarrow H_2O(m,n)+X$ reaction, where X is Cl or Br. Most of the details of the theory are presented in Ref. 5. The vector joining the centers of mass of the OH and HX molecules is denoted $\mathbf{R}_1$ and the vector between the H and O atoms of OH is $\mathbf{R}_2$. The vector $\mathbf{R}_3$ that joins the H and X atoms of HX has an angle γ with respect to $\mathbf{R}_1$. The angle between $\mathbf{R}_1$ and $\mathbf{R}_2$ is θ and the torsional angle between $\mathbf{R}_2$ and $\mathbf{R}_3$ is ϕ. In the RBA, $\mathbf{R}_3$ is aligned along $\mathbf{R}_1$ so that γ and ϕ are set to zero. However, the zero-point energies associated with the γ and ϕ motions are calculated and these adiabatic energies are added to the potential energy surface as described below (this aspect of the theory was not applied explicitly in Ref. 5).

We have found in previous calculations on the related $OH+H_2$ reaction that it is an excellent approximation[7] to freeze the OH bond in the dynamics calculations. Cross sections into the local OH stretching quantum number n of product $H_2O(m,n)$ then refer to the sum over cross sections into both the symmetric and asymmetric stretch vibrations of H_2O. A "spectator bond" behavior was also found[26] in calculations on the $CN+H_2\rightarrow HCN+H$ reaction, and seems to apply to many reactions of polyatomic molecules.

We use the coordinates

$$s_i^2=\frac{M_i}{\mu}R_i^2, \quad i=1 \text{ and } 3$$

with the hyperspherical transformation

$$s_1=\rho\cos(\delta), \quad s_3=\rho\sin(\delta),$$

where

$$\mu=(M_1M_2M_3)^{1/3},$$

$$M_1=[(m_O+m_H)(m_H+m_X)]/(m_O+2m_H+m_X),$$

$$M_2=m_Om_H/(m_O+m_H), \quad M_3=m_Hm_X/(m_H+m_X),$$

and the masses of the O, H, and X atoms are m_O, m_H, and m_X, respectively.

The Hamiltonian H is a function of the three variables ρ, δ, and θ,

$$H=-\frac{\hbar^2}{2\mu}\frac{\partial^2}{\partial\rho^2}-\frac{\hbar^2}{2\mu\rho^2}\frac{\partial^2}{\partial\delta^2}+\left(\frac{\hbar^2}{2MR^2}\right)(j_2^2-K^2)+Bj_2^2+\frac{\hbar^2}{2\mu\rho^2}\left[J(J+1)-K^2+\frac{3}{4}\right]+V(\rho,\delta,\theta), \tag{1}$$

where $M=m_H(m_O+m_H)/(2m_H+m_O)$, V is the potential energy surface, B is the rotor constant of OH, and R is the distance from the bond-breaking H atom of H_2O to the center of mass of OH. Also j_2^2 is the operator associated with the rotation of OH, J is the total angular momentum, and K, which is assumed to be conserved,[5,21] is the projection of both $\mathbf{j}_2$ and $\mathbf{J}$ along the intermolecular axis $\mathbf{R}_1$.

The R-matrix propagator method[27] is employed to solve the coupled-channel equations for the Hamiltonian of Eq. (1) with a fixed total energy E and total angular momentum J and projection quantum number K. This requires the hyperradius ρ to be divided up into sectors with midpoints $\{\rho_i\}$. The wave function in sector i for initial quantum state labeled by k' is expanded in the coupled-channel form

$$\Psi_{k'}(\rho,\delta,\theta;\rho_i)=\sum_k^N f_{kk'}(\rho;\rho_i)\psi_k(\delta,\theta;\rho_i). \tag{2}$$

The $[\psi_k(\delta,\theta;\rho_i)]$ functions are computed by diagonalizing the Hamiltonian (1) for $\rho=\rho_i$ with

$$\psi_k(\delta,\theta;\rho_i)=\sum_{k_1}^{N_\delta}\sum_{k_2}^{N_\theta}c_{k_1k_2}^k(\rho_i)\psi_{k_1}(\delta;\rho_i)\psi_{k_2}(\theta;\rho_i). \tag{3}$$

The energies $[E_k(\rho_i)]$ obtained from this diagonalization give the so-called hyperspherical adiabats when plotted vs ρ.[16]

The functions $[\psi_{k_1}(\delta;\rho_i)]$ of Eq. (3) are calculated by diagonalizing the Hamiltonian

$$H=-\frac{\hbar^2}{2\mu\rho_i^2}\frac{\partial^2}{\partial\delta^2}+V_0(\delta;\rho_i) \tag{4}$$

with a basis set of n_δ equally spaced distributed Gaussian functions.[28] An appropriate potential $V_0(\delta;\rho_i)$ is obtained by using the equilibrium bond angle θ_{eq} of H_2O in $V(\rho_i, \delta, \theta_{eq})$. Examination of $V_0(\delta;\rho_i)$ as a function of δ gives a double-minimum potential for larger values of ρ. For large ρ, a local minimum for small δ gives the energy levels of the OH(j) +HX(v) reactants and a local minimum for a larger value of δ gives the vibrational levels of the $H_2O(m,n)$ product. This double minimum has a maximum "ridge" energy $r(\rho_i)$ between the two local minima. The ridge energy is very useful[16,29,30] in understanding the vibrationally selected reaction probabilities and is discussed in more detail below.

The functions $[\psi_{k_2}(\theta;\rho_i)]$ are expanded as a linear combination of n_θ spherical harmonics $[Y_j^K(\theta,0)]$ and are obtained from diagonalization of the Hamiltonian

$$H=\left(\frac{\hbar^2}{2MR^2}\right)(j_2^2-K^2)+Bj_2^2+V_1(\theta;\rho_i), \tag{5}$$

where

$$V_1(\theta;\rho_i)=\langle\psi_1(\delta;\rho_i)|V(\rho_i,\delta,\theta)|\psi_1(\delta;\rho_i)\rangle. \tag{6}$$

B. Reaction probabilities and cross sections

The close-coupled equations are solved[27] by propagating the R matrix from a small value of $\rho=\rho_S$, to a large value $\rho=\rho_L$. Scattering boundary conditions are then applied when the interaction between the reactant and product channel becomes negligible. The S-matrix elements $S_{vj,mn}^{J,K}(E)$ are obtained for the state-selected transition in the reaction $OH(j,K)+HX(v)\rightarrow H_2O(m,n,K)+X$. Note that the quantum number K can be identified approximately with a rotational state of the H_2O molecule as described in Ref. 21. The state-selected reaction probabilities are

$$P_{vj,mn}^{J,K}(E)=|S_{vj,mn}^{J,K}(E)|^2.$$

From these, the state-selected integral reaction cross sections are obtained as

$$\sigma(v,j,K\rightarrow m,n)=\frac{\pi}{k_{vj}^2}\sum_J(2J+1)P_{vj,mn}^{J,K}(E),$$

$$\sigma(v,j\rightarrow m,n)=\frac{1}{(2j+1)}\sum_{K=-j}^{j}\sigma(v,j,K\rightarrow m,n),$$

$$\sigma(v,j)=\sum_{m,n}\sigma(v,j\rightarrow m,n), \tag{7}$$

where

$$k_{vj}^2=\frac{2M_1}{\hbar^2}(E-E_v-E_j)$$

and E_v and E_j are the energies of the initial HX vibrational state v and OH rotational state j. The initial translational energy for the (v,j) state is given by $E_{trans}=E-E_v-E_j$.

The rotational motion of the HX molecule is not treated explicitly in the scattering calculations. This can be compensated for in two different ways. In the energy shift approximation,[31] the in-plane (ϵ_{in}) and out-of-plane (ϵ_{out}) bending energies of the HX molecule at the transition state of the reaction are calculated and used to correct the collision energy as described in Ref. 5. A more accurate "adiabatic bend" procedure can be used that follows the approach of Bowman and co-workers.[31] First, the potential energy surface is minimized with respect to the angles γ and ϕ for fixed values of ρ, δ, and θ to give V_m (ρ,δ,θ). Then the harmonic zero-point energies for the in-plane (γ) and out-of-plane (ϕ) bending vibrations of the OHHX complex that correlate with HX motion are added to $V_m(\rho,\delta,\theta)$ to give the potential $V(\rho,\delta,\theta)$ that is used in the Hamiltonian of Eq. (1). The harmonic energies associated with the bending of HX were calculated by applying the FG-matrix method[32] for the three bending degrees of freedom in the OHHX complex and identifying the mode with largest frequency as the H_2O bend (which also correlates with OH bending motion). This adiabatic bend approach is used in all the rate constant and cross section calculations reported here,

Strictly speaking, the collision cross sections should also be summed over all open HX bending states at the transition state to give "rotationally averaged" cross sections that refer to an averaged sum over all initial rotational states of HX.[31] However, since the vibrational product distributions are very insensitive to collision energy in the low energy range considered here, this sum was not carried out for the cross sections reported in the figures here (although this effect is included in the rate constant calculations as described below).

C. Rate constants

Rate constants are calculated by adapting a procedure that has been shown to be quite accurate by comparison with accurate quantum scattering results of cumulative rate constants for the $OH+H_2$ reaction.[5,17] First, the rate constant $k'(T)$ is calculated by Maxwell–Boltzmann averaging the product of the initial velocity and the cross sections $\sigma(v,j)$ of Eq. (7), with $v=0$, $j=0$, and $K=0$. The rate constant for HCl+OH ($j=0$, $K=0$) is then calculated as

$$k_0(T)=\frac{k'(T)}{\{1-\exp[-(2\epsilon_{in})/(k_\beta T)]\}\{1-\exp[-(2\epsilon_{out})/(k_\beta T)]\}\{1+\exp[-(\Delta E)/(k_\beta T)]\}}, \tag{8}$$

where k_β is the Boltzmann constant and the term in curly brackets arises as the two electronic states of OH $^2\Pi_{3/2}$ and $^2\Pi_{1/2}$ can both be populated and are separated by an energy of ΔE. In this expression, it has been necessary to sum over all excited bending states of HCl at the transition state.[5]

For OH+HBr, the transition state is not well-defined and cross sections are summed over those obtained in separate calculations in which the energies of both ground and excited states of the harmonic in-plane (γ) and out-of-plane (ϕ) bending vibrations of the OHHX complex are added to $V_m(\rho,\delta,\theta)$. The rate constant $k_0(T)$ is then calculated from an equation analogous to Eq. (8) but without the terms containing ϵ_{in} and ϵ_{out}.

The calculations reported in Sec. V show that the cross sections at small translational energies for both OH+HCl and OH+HBr with $|K|=j$ are close in magnitude to those for ($j=0$, $K=0$) and the cross sections for $j>|K|$ are much smaller than those for $j=|K|$. This suggests that, at lower temperatures, the degeneracy averaged rate constant k_j is obtained as

$$k_j(T)=\frac{2k_0(T)}{(2j+1)}, \quad (j\neq 0), \tag{9}$$

where the factor of 2 arises as K ranges from $-j$ to $+j$ and the Hamiltonian is independent of the sign of K. Maxwell–Boltzmann averaging $k_j(T)$ over all j then gives the final rate constant as

$$k(T)\approx\frac{k_0(T)\{1+2\Sigma_{j=1}\exp[-E_j/(k_\beta T)]\}}{\Sigma_{j=0}(2j+1)\exp[-E_j/(k_\beta T)]}\approx k_0(T)\sqrt{\frac{B\pi}{k_\beta T}}, \tag{10}$$

where B is the rotor constant of the HX molecule. It should be noted that if $k_0(T)$ does not have a strong temperature dependence (as is the case in the OH+HBr reaction), then the $T^{-1/2}$ dependence will dominate the temperature dependence of $k(T)$ at lower temperatures.

D. Hyperspherical adiabats

The hyperspherical adiabats tend to the energies $[E_k(\rho)]$ associated with either the reactant (j,K,v) or product (m,n) channels for large ρ. It is known from atom–diatom studies that asymptotic quantum numbers are particularly good labels of the hyperspherical adiabats for heavy–light–heavy reactions.[30] This is because the hyperspherical coordinate transformation for these reactions produces a "light particle" motion δ and a "heavy particle" motion ρ, which have very different time scales. If two of the hyperspherical adiabats correlating with different arrangement channels exhibit an avoided crossing at an energy close to the ridge energy $r(\rho)$, then chemical reaction between the two quantum states that label these adiabats will have an appreciable probability. Therefore, plots of $[E_k(\rho)]$ and $r(\rho)$ on the same diagram immediately indicate which quantum states in reactants and products are likely to have the largest reaction probabilities. This is examined in detail for the reactions considered here and provides an explanation for many of the calculated reaction propensities involving both vibrational and rotational states.

TABLE I. Morse and Sato parameters in the LEPS potential energy surfaces for the OH+HX reactions (in atomic units).

X	Parameter	O–H	H–X	O–X
Cl	β^a	1.214	0.989	1.212
	$D_e{}^a$	0.1698	0.1697	0.1031
	$r_e{}^a$	1.833	2.4093	2.967
	Δ^b	0.112	0.112	0.112
	c^c		0.024	
Br	β	1.214	0.958	1.30
	D_e	0.1698	0.1441	0.0899
	r_e	1.833	2.672	3.245
	Δ	0.112	0.112	0.112
	c		0.024	

[a]Morse parameters.
[b]SATO parameter.
[c]Damping coefficient in potential energy expansion of Eq. (11). Note that in Ref. 21, $c=0.022$ was used.

III. POTENTIAL ENERGY SURFACES

For both HX+OH′ reactions, with X=Cl and Br, the potential energy surfaces are

$$V=V_{\rm LEPS}(r_{\rm OH},r_{\rm HCl},r_{\rm OCl})+V_{\rm H_2O}(r_{\rm OH},r_{\rm OH'},r_{\rm HH'})$$
$$-V_{\rm OH}(r_{\rm OH})+[\tanh(cr_{\rm XH'}^2)-1]V_{\rm HH'}(r_{\rm HH'}). \tag{11}$$

Here, r_{AB} is the distance between atoms A and B, $V_{\rm LEPS}$ is a LEPS potential appropriate for the O+HX→OH+X reaction[33,34] and $V_{\rm H_2O}$ is a potential for H_2O of Murrell and Carter[22] that gives the correct vibrational states of H_2O and also gives a realistic description of the breaking of all the bonds in H_2O. Since there is a two-body potential for the OH bond present in both $V_{\rm LEPS}$ and $V_{\rm H_2O}$, the two-body term $V_{\rm OH}$ in $V_{\rm H_2O}$ is subtracted out. Also, the interaction potential between the two hydrogen atoms $V_{\rm HH'}$ in $V_{\rm H_2O}$ is too attractive to allow for a realistic transition state and so this term is damped by the tanh function that contains a single parameter c and depends on the distance squared between the X atom and the spectator atom H′. This damping function ensures that the vibrational energy levels of H_2O are not affected when the X atom is at a large distance from H_2O. In the potential for H_2O of Ref. 22, there is a term in $(r_{\rm HH'})^2(r_{\rm OH}^2+r_{\rm OH'}^2)$ that gives an unphysical contribution to the HXOH′ potential when $r_{\rm HH'}$ and $r_{\rm OH}$ or $r_{\rm OH'}$ are quite large. This term is omitted from $V_{\rm H_2O}$ in Eq. (11) and it is found that this has an insignificant effect on the calculated vibrational frequencies for H_2O.

It should be emphasized that this form of potential energy function is probably an oversimplification of the problem. However, it does give the energetics and rovibrational energy levels of the reactants and products correctly and also gives reasonable rate constants. In studying the vibrationally selected reactions at a qualitative level, this form of potential should be reasonable.

Table I gives the Morse parameters used in $V_{\rm LEPS}$ for both the OH+HCl and OH+HBr reactions together with the Sato parameters and damping parameters c. For OH+HCl, the Morse and Sato parameters in $V_{\rm LEPS}$ determined by Persky and Broida were used.[33] These parameters were obtained

TABLE II. Transition state geometries and vibrational frequencies for the OH+HCl reaction obtained with the UHF method and the potential energy surface of Eq. (11).

Coordinate	UHF	Equation (11)	Vibrational symmetry	Frequency (UHF) (cm^{-1})	Frequency equation (11) (cm^{-1})
R_{HCl}	1.496 Å	1.429 Å	A'	350	394
R_{HO}	1.164 Å	1.169 Å	A'	729	597
$R_{H'O}$	0.951 Å	0.978 Å	A'	1294	1670
∠HOH′	105.3°	110.0°	A'	4073	3604
∠ClHO	159.5° [a]	167.2° [a]	A''	363	590

[a]In the UHF calculation, the ClHOH transition state is a *cis* structure, while in the fit of Eq. (11), the structure is *trans*. However, in both cases, the geometry of the ClHO at the transition state is close to linear (i.e., the ClHO angle is close to 180°).

by comparing quasiclassical trajectory calculations with experimental rate constants for the O+HCl→OH+Cl reaction. For OH+HCl, the damping coefficient c was varied until the geometry of the transition state of the reaction agreed reasonably well with the transition state obtained from an *ab initio* calculation which is described below.

Except for the Sato parameter, the parameters in V_{LEPS} of the OH+HBr reaction were also chosen to be the same as those obtained from quasiclassical trajectory comparisons[34] with experiment for the O+HBr→OH+Br reaction. *Ab initio* calculations are not reported for OH+HBr, and the same Sato parameter in V_{LEPS} and c coefficient were used as for OH+HCl. The potential energy surface for the OH+HBr reaction has no classical barrier.

The potential energy surfaces give bending and local OH stretching frequencies for isolated H_2O of 1612 and 3701 cm^{-1}, respectively. These results should be compared with the experimental[35] H_2O vibrational frequencies of 1595, 3657, and 3756 cm^{-1} for the bend, symmetric, and asymmetric stretch vibrations, respectively.

Some limited *ab initio* calculations were done on the OH+HCl transition state. Qualitative molecular orbital considerations indicate that a single configuration wave function properly represents this transition state. There are two relevant orbitals involved in the reaction—a singly occupied orbital (in the OH radical for reactants and in the Cl radical for products) and the bond transferred during the reaction (HCl bond in reactants and the new OH bond in products). The transformation of reactants to products is accompanied by a change in the nature of these two orbitals and not a change in electronic configuration. On the other hand, as has been noted in the related H_2+OH reaction,[36] spin recoupling must be treated for a more quantitative description of the transition state structure.

On the basis of the above considerations, we have selected an unrestricted Hartree–Fock (UHF) wave function to predict the geometry and harmonic frequencies of the transition state for OH+HCl. Spin contamination did not prove to be a serious problem for this system ($\langle S^2\rangle$=0.8). All calculations have been performed with Gaussian 90 using the standard basis set 6-311++G(d,p), which includes two diffuse and one polarization function per atom.[37] The transition state is reported in Table II.

The transition state structure for OH+HCl is planar and has an electronic and spin symmetry of $^2A'$. This *ab initio* data is only expected to be a qualitative guide for assisting in the construction of the potential energy surface for use in dynamics calculations. In particular, as expected, the calculated barrier height at the transition state is much too large—8647 cm^{-1} at the UHF level of theory and 2521 cm^{-1} when correlation is included at the second-order unrestricted Møller–Plesset (UMP2) level.

In the OH+HCl channel, configurations close to linear are favored through the strong dipole–dipole interactions. At these geometries, the electronic and spin symmetry of the system is $^2\Pi$. Bending of the complex is necessary to reach the saddle point and at these geometries the previously degenerate state splits into A' and A'' components. At the saddle point, the electronic energy of the A'' state is 6960 cm^{-1} (UHF) and 4134 cm^{-1} (UMP2) above the A' state and therefore the A'' potential energy surface was not explored further.

Also shown in Table II are the transition state geometry and vibrational frequencies obtained in the simple potential energy fit of Eq. (11). It can be seen that the overall agreement with the UHF data is quite good considering that there was only one variable parameter (c) in the potential energy surface expansion. Note that the bending frequency of H_2O at the transition state is high in both the UHF calculation (1294 cm^{-1}) and potential fit (1670 cm^{-1}). Also, the OH spectator bond length at the transition state in both the UHF calculation and the potential fit is close to the value for isolated OH of 0.970 Å. Furthermore, in both the UHF calculation and potential fit, the geometry of the transition state is close to a structure in which the ClHO geometry is linear. The fitted potential gives a very small classical barrier of 86 cm^{-1} at the transition state. However, the addition of the zero-point energies of the bending modes does ensure a larger effective barrier than this.

TABLE III. Parameters used in the rotating bond calculations.

Reaction	ρ_S (a.u.)	ρ_L (a.u.)	n_δ	n_θ	N_δ	N_θ	N
OH+HBr	8.5	33.9	98	18	18	18	70
OH+HCl	8.5	34.9	98	18	18	18	30

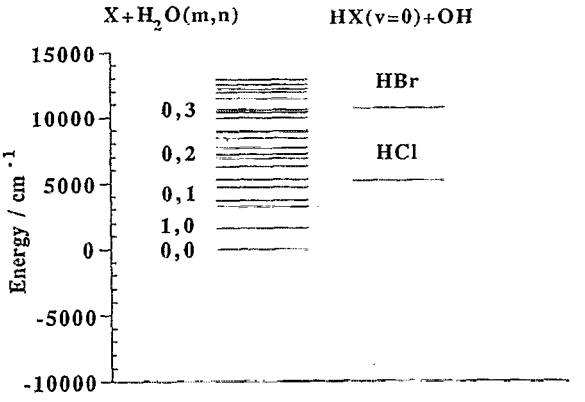

FIG. 1. Energies of the $X+H_2O(m,n)$ states and the $HX(v=0)+OH(j=0)$ states with X=Cl and Br.

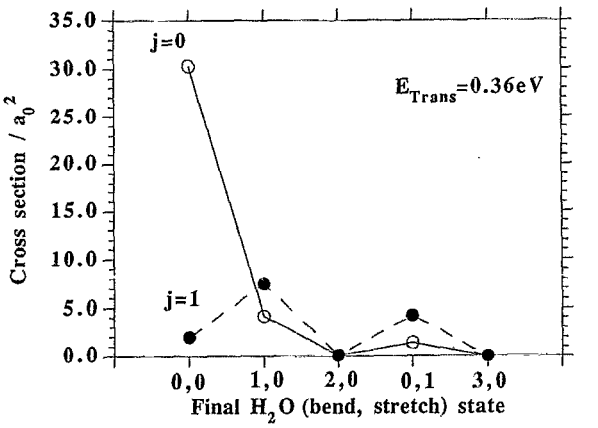

FIG. 2. Cross sections for the $HCl(v=0)+OH(j,K=0)\rightarrow Cl+H_2O(m,n)$ reaction plotted against product state (m,n) with $j=0$ and 1 and initial translational energy of 0.36 eV. Note that m is a vibrational bending quantum number and n is a local OH stretching quantum number of H_2O.

IV. NUMERICAL DETAILS

The parameters needed to get numerically converged cross sections are similar to those needed for the $OH+H_2$ reaction[5] and are listed in Table III. Typically about 120 R-matrix sectors and up to 150 values of J were needed to get converged cross sections at the thermal energies that were considered. On the basis of our convergence tests, we expect the cross sections reported here to be converged numerically to within 10%. The potential surface for OH+HCl gave the HCl transition state bending frequencies of $\epsilon_{in}=597$ cm^{-1} and $\epsilon_{out}=590$ cm^{-1}.

V. ROVIBRATIONALLY SELECTED DYNAMICS

Figure 1 gives a diagram of the energies of the $HX(v=0)+OH$ channel compared to that for the $X+H_2O(m,n)$ channel. It can be seen that the $OH+HBr\rightarrow H_2O+Br$ reaction is very exothermic, while $OH+HCl\rightarrow H_2O+Cl$ is quite exothermic. This means that a much larger number of vibrational states of H_2O can be populated in the HBr reaction than in HCl. This has consequences for the vibrationally selected reaction dynamics that are discussed below.

A. Cross sections for OH+HCl

Figure 2 shows calculated cross sections for the $OH(j,K=0)+HCl(v=0)\rightarrow H_2O(m,n)+Cl$ reaction at a collision energy of 0.36 eV. It can be seen that the product ground state (0,0) of H_2O has by far the largest cross section for reaction out of $j=0$, while the state (1,0) with one quantum of energy in the first excited bending mode of H_2O is favored for reaction from $(j=1, K=0)$. This finding can easily be explained by examination of the hyperspherical adiabat plots of Fig. 3 for $K=0$. Here it can be seen that the avoided crossing at $\rho_c\approx 12$ a.u. of the vibrationally selected adiabats correlating with $OH(j=0, K=0)+HCl(v=0)$ and $Cl+H_2O(0,0)$ also coincides with the value of the ridge energy $r(\rho_c)$ at $\rho=\rho_c$, while the $OH(j=1, K=0)+HCl(v=0)$ adiabat has an avoided crossing with that for $Cl+H_2O(1,0)$. A result of this is that reaction out of $(j=0, K=0)$ has very little activation energy, while that out of $(j=1, K=0)$ has an activation energy roughly correlating with the first excited bending energy of H_2O of 0.2 eV. This is seen clearly in Fig. 4, where the cross sections out of $OH(j,K=0)$ with $j=0$ and 1 are compared as a function of collision energy; the $j=1$ cross sections, which are much smaller than those for $j=0$ over the entire energy range, do increase sharply in magnitude at translational energies above 0.2 eV.

Figure 5 compares cross sections for reaction out of $OH(j=2,3, K=2)$ with those for $(j=0,1, K=0)$. It can be seen that the cross sections for $(j=2, K=2)$ are close to those for $(j=0, K=0)$, while those for $(j=3, K=2)$ and $(j=1, K=0)$ are much smaller. This is explained by the hyperspherical plots for the $K=2$ states of Fig. 6 which look almost identical to those for $K=0$ of Fig. 2 except that the lowest adiabat of OH correlates with $(j=2, K=2)$ in Fig. 6 instead of $(j=0, K=0)$ of Fig. 2. It can be seen that the adiabat correlating with $(j=2, K=2)$ has an avoided crossing with that for $H_2O(0,0)$. This marked rotational effect suggests that the K-averaged cross sections are given approximately by

$$\sigma(v,j)=\frac{1}{2j+1}\sum_{K=-j}^{j}\sigma(v,j,K)$$

$$\approx\frac{2}{2j+1}\sigma(v,j=0,K=0)\quad(j\neq 0),$$

where the factor of 2 arises because the cross sections for $K=-j$ are identical to those for $K=j$. This new effect also gives rise to the simple form of the rate constant discussed in Sec. II C. Strong rotational effects have also been seen in quantum scattering calculations[38] on three-atom heavy–light–heavy reactions such as Cl+HCl, although the dynamics of that reaction is somewhat different to those considered here.

B. Cross sections for OH+HBr

Figure 7 gives the calculated cross sections for the $OH(j=0, K=0)+HBr(v=0)\rightarrow H_2O(m,n)+Br$ reaction at a collision energy of 0.06 eV. Here it can be seen that several

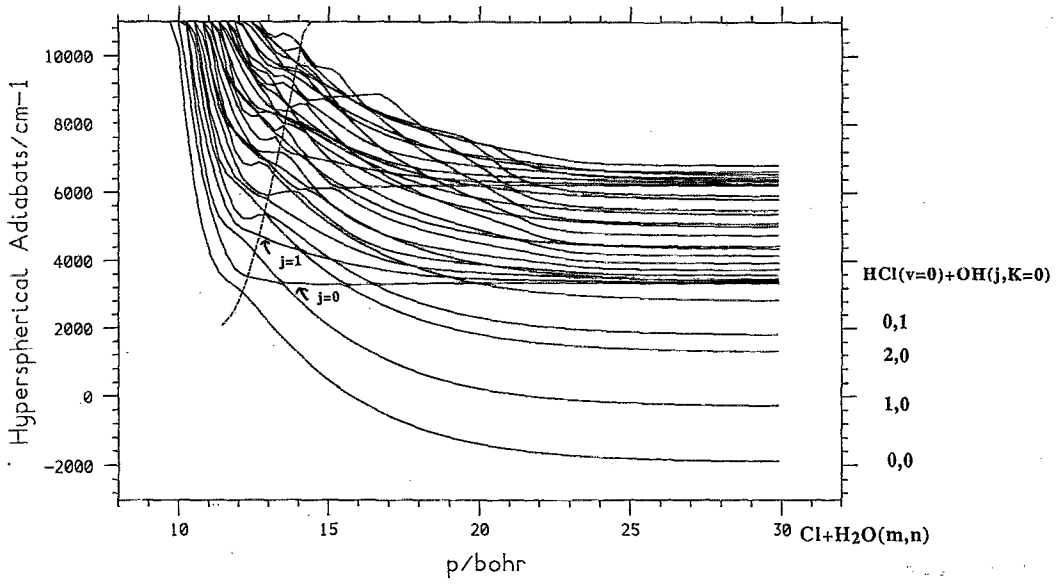

FIG. 3. A plot of the hyperspherical adiabats for the $HCl(v)+OH(j,K=0)\rightarrow Cl+H_2O(m,n)$ reaction. Note the avoided crossing between the $HCl(v=0)+OH(j=0)$ and $Cl+H_2O(0,0)$ channels in the region of the ridge $r(\rho)$ (broken line).

product vibrational states of H_2O are populated, but the state (1,1) with one quantum of energy in the bending mode and one quantum in the local OH stretch has the largest cross section. Yet again, this finding is explained well by examination of the hyperspherical adiabat plots of Fig. 8 for $K=0$. Here it can be seen that the ridge $r(\rho)$ crosses the $OH(j=0, K=0)+HBr(v=0)$ adiabat at a position very close to its avoided crossing with the adiabat correlating with $H_2O(1,1)+Br$. Unlike the OH+HCl reaction, however, there are other vibrational states of H_2O that are quite close to this crossing point, such as $H_2O(2,1)$ and $H_2O(0,2)$, and these product states are also populated. One quantum in the local stretching state of H_2O corresponds in our calculation to a sum of reaction into one quantum in the asymmetric and symmetric stretch vibrations of three-mode H_2O. Therefore, our findings suggest that the most likely product states of H_2O that will be experimentally observable will be the vibrations (1,1,0) and (0,1,1) in the full triatomic normal-mode notation of (symmetric stretch, bend, asymmetric stretch).

The OH+HBr reaction shows a similar dependence on $OH(j,K)$ as was found for OH+HCl. The cross sections for $OH(j,K=j)$ are large and close to those for $(j=0, K=0)$, while those for $j>|K|$ are much smaller. This is illustrated in Fig. 9. Note that the cross sections for this reaction are very large even at very low collision energy as, unlike OH+HCl, there is no barrier to reaction in the potential energy surface.

C. Rate constants for OH+HCl and OH+HBr

Rate constants were calculated from the cross sections using the procedures described in Sec. II C. The cross sections were calculated at a range of energies sufficient to give

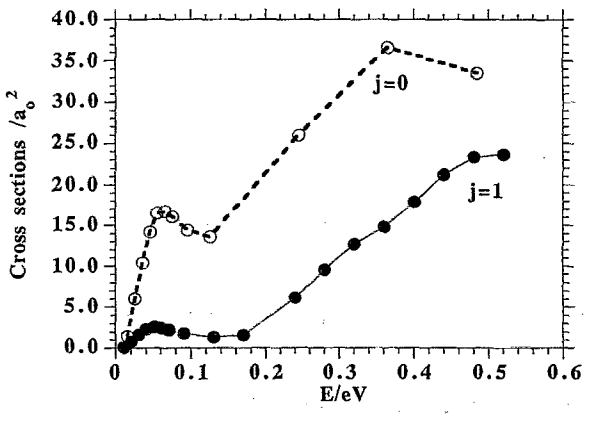

FIG. 4. Cross sections for the $HCl(v=0)+OH(j,K=0)$ reaction, with $j=0$ and 1, summed over all product states and plotted as a function of initial translational energy.

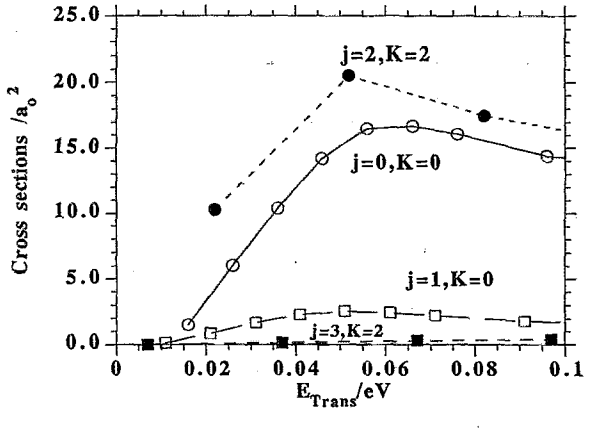

FIG. 5. Cross sections for the $HCl(v=0)+OH(j,K)$ reaction, with $K=0$ and $K=2$, summed over all product states and plotted as a function of initial translational energy.

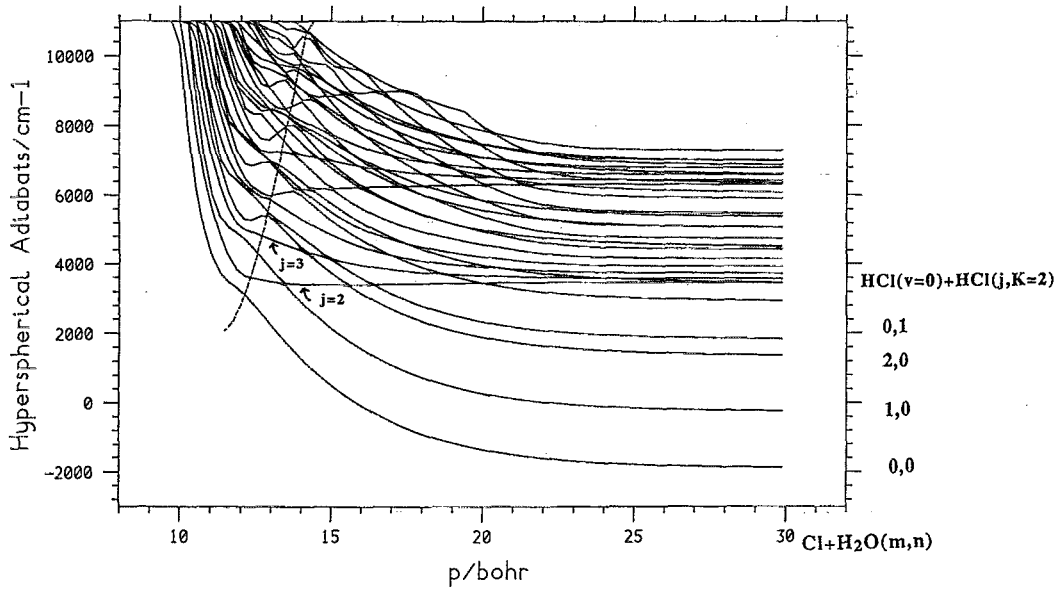

FIG. 6. A plot of the hyperspherical adiabats for the $HCl(v)+OH(j,K=2)\rightarrow Cl+H_2O(m,n)$ reaction. Note the avoided crossing between the $HCl(v=0)+OH(j=2,K=2)$ and $Cl+H_2O(0,0)$ channels in the region of the ridge $r(\rho)$ (broken line).

rate constants at temperatures of 300 K and below for both the OH+HCl and OH+HBr reactions. A comparison of the calculated rate constants with the experimental results[14,15,39] is shown in Fig. 10. It can be seen that the agreement with experiment is quite good for the OH+HCl reaction, with the calculated values agreeing to within a factor of 2. In the case of the OH+HBr reaction, the calculated rate constant is slightly below experiment,[14] but the negative temperature dependence of the rate constants is obtained. As is explained in Secs. II C and V A, this negative temperature dependence results directly from the degeneracy averaged rate constants $k_j(T)$ and cross sections $\sigma(v=0,j)$ having the $(2j+1)^{-1}$ dependence.

As can be seen from Fig. 9, the reaction cross sections for the OH+HBr reaction have only a slight dependence on collision energy and the $k(j=0)$ rate constant for this reaction has hardly any temperature dependence, apart from that arising from the electronic partition function for the reaction [see Eq. (8)]. The rate constant formula of Eq. (10) then suggests a general form of rate constant for this reaction

$$k(T)=\frac{A}{T^{1/2}[1+\exp(-181/T)]}, \tag{12}$$

where A is a parameter and the difference between the $^2\Pi_{3/2}$ and $^2\Pi_{1/2}$ electronic states of OH is 181 K. Figure 11 shows a fit of Eq. (12) to the experimental rate constants and the agreement is quite good. We therefore believe that our theory gives a simple explanation of the strong negative temperature dependence of the rate constant for the OH+HBr reaction in terms of the dependence of the rotationally selected reaction cross sections on $(2j+1)^{-1}$. In turn, the underlying reason for this effect is the large bending frequency of H_2O at the transition state.

The rotationally adiabatic capture theory with a dipole-dipole potential gives a maximum of 3.5×10^{-10} $cm^3\ s^{-1}$ molecule^{-1} for the rate constant of the OH+HBr reaction[24] at a temperature of 20 K. This theory also predicts that the rate constant should have a $T^{1/6}$ (i.e., positive) temperature dependence in the very low temperature region (below 10 K). The experimental rate constants for this reaction have been measured down to 23 K, where the rate constant is[14] 1.07×10^{-10} $cm^3\ s^{-1}$ molecule^{-1}. It would be very interesting if the experiments could be done for even lower temperatures to see if the theoretically predicted[24] maximum in the rate constant is observed. In the very low temperature region (less than ~10 K), the rotationally adiabatic capture theory might be more accurate than the theory described here as it explicitly takes into account the open-shell nature of the OH radical and treats the very long range part of the potential energy surface accurately.

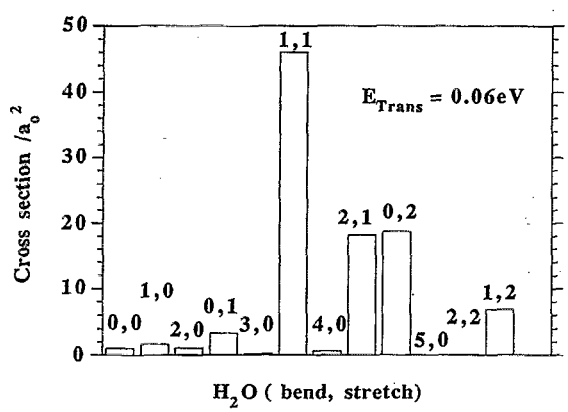

FIG. 7. Cross sections for the $HBr(v=0)+OH(j,K=0)\rightarrow Br+H_2O(m,n)$ reaction plotted against product state (m,n) and initial translational energy of 0.06 eV.

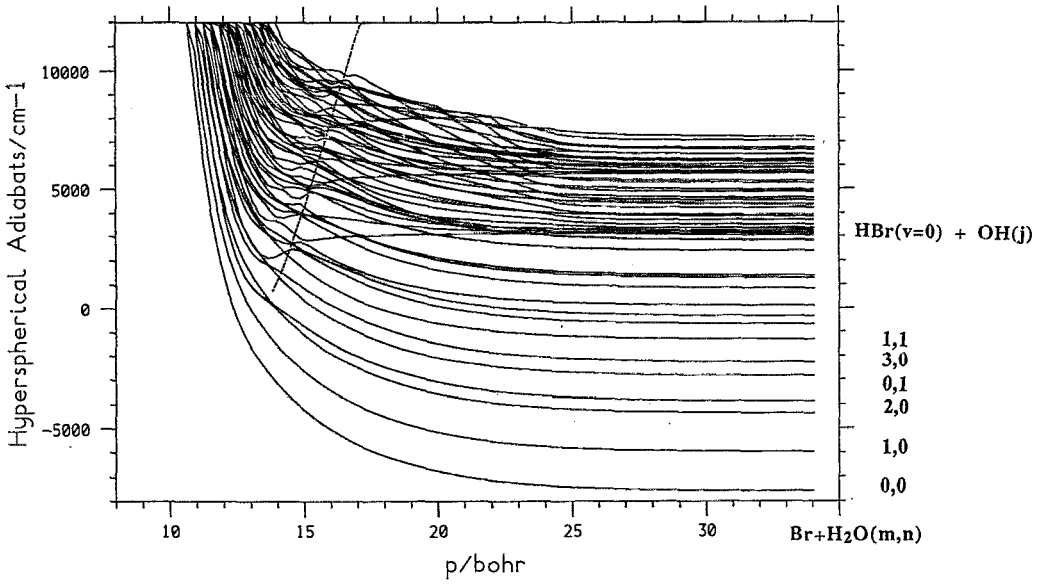

FIG. 8. A plot of the hyperspherical adiabats for the $HBr(v)+OH(j,K=0)\rightarrow Br+H_2O(m,n)$ reaction. Note the avoided crossing between the $HBr(v=0)+OH(j=0,K=0)$ and $Br+H_2O(1,1)$ channels in the region of the ridge $r(\rho)$ (broken line).

In the case of the OH+HCl reaction, $k_{j=0}(T)$ has a small activation energy which is balanced by the $T^{-1/2}$ term at lower temperatures, so that the temperature dependence of $k(T)$ is very flat. We have not performed calculations at higher energies to examine the rate constant at higher temperatures. At higher temperatures, the rate constant for the OH+HCl reaction is observed to increase more sharply with temperature and an activation energy is apparent.[39] This could be related to reaction via the transition state with the first excited bending mode of H_2O which becomes energetically accessible at higher energies. This would suggest that Eq. (10) might need to be modified for higher temperatures to a form such as

$$k(T)=k_0(T)\left[1+\exp\left(-\frac{E_b}{k_\beta T}\right)\right]\sqrt{\frac{B\pi}{k_\beta T}},$$

where E_b is the bending energy of H_2O at the transition state of the reaction.

The rate constant of Eq. (10) also suggests a simple $B^{1/2}$ dependence on the rotor constant of OH. In experimental measurements, Smith and Williams[40] have determined the ratio between the rate constants for the OH+HCl and OD+HCl reactions at 298 K to be 1.5, and this is in good agreement with the $B^{1/2}$ dependence of our theory that gives a ratio of 1.4. It would be interesting if the same ratio could be measured for the OH+HBr and OD+HBr reactions. We note also that there are other heavy–light–heavy reactions involving neutral polyatomic molecules that show a strong negative temperature dependence in the experimentally determined rate constants at lower temperatures, an example being the $CN+NH_3$ reaction.[41] It could be that the findings described here are relevant for understanding the temperature

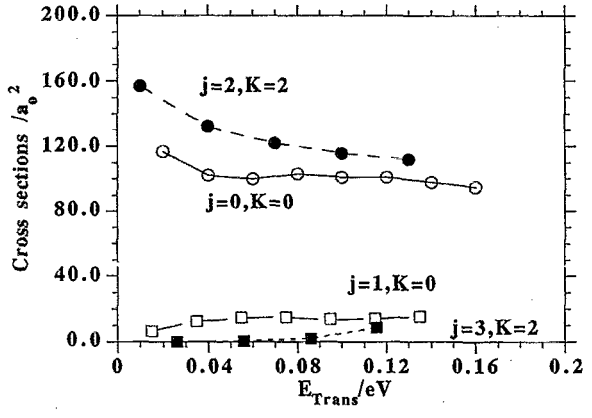

FIG. 9. Cross sections for the $HBr(v=0)+OH(j,K)$ reaction, with $K=0$ and $K=2$, summed over all product states and plotted as a function of initial translational energy.

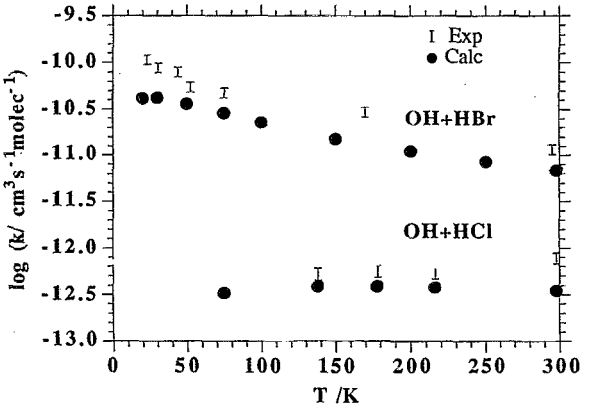

FIG. 10. Calculated rate constants for the OH+HCl and OH+HBr reactions compared with the experimental (Refs. 14 and 15) results.

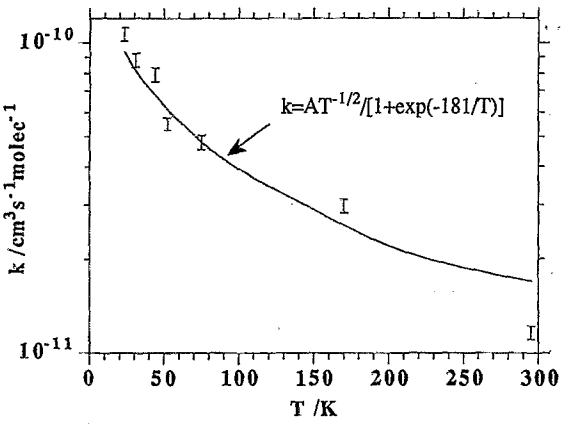

FIG. 11. A fit of the rate constant expression (12) to the experimental results (Ref. 14) (error bars) for the OH+HBr reaction.

dependence of the rate constants for other reactions such as this.

VI. CONCLUSIONS

The rotating bond approximation has been used in quantum scattering calculations on the reactions $OH+HCl \rightarrow H_2O+Cl$ and $OH+HBr \rightarrow H_2O+Br$ for thermal collision energies. Simple potential energy surfaces have been constructed for these reactions based on a LEPS function and an accurate H_2O potential. These potentials have the correct reactant and product energies and, in the case of OH +HCl, the transition state geometry is in reasonable agreement with *ab initio* data. The potentials are only expected to be of qualitative accuracy, but are still useful in examining the general features of the rovibrationally selected dynamics in these reactions.

It is found in the calculations on the OH+HCl reaction that the vibrational ground state is the most likely product vibrational state of H_2O produced in the reaction. This is explained by examination of the vibrationally adiabatic potential curves expressed in hyperspherical coordinates which show a strongly avoided crossing between the reactant $OH(j=0)+HCl(v=0)$ and product $Cl+H_2O(0,0)$ channels. In the computations on OH+HBr, the most likely product vibrational state has one quantum in the H_2O bend and one quantum in the local OH stretch of H_2O. This is explained through a strongly avoided crossing between the hyperspherical adiabats correlating with $OH(j=0)+HBr(j=0)$ and $Br+H_2O(1,1)$.

A particularly striking effect that is found in the computations on both reactions is the dependence of the rotationally selected cross sections and rate constants on $(2j+1)^{-1}$, where j is the OH rotational quantum number. This is due to the strong correlation between the (j,K) states and the ground and excited bending states of H_2O. For example, $(j=0, K=0)$ gives reaction mainly into the ground vibrational state of H_2O, while $(j=1, K=0)$ gives reaction mainly into the first excited bending vibration of H_2O and hence has a significant activation energy. This is a new effect which is related to the strongly adiabatic nature of these four-atom heavy–light–heavy reactions and presents an interesting experimental challenge in its detailed verification.

The strong rotational effect produces a simple form for the rate constants for these reactions which includes a $(B/T)^{1/2}$ factor. This would appear to explain well the marked negative temperature dependence observed in the rate constants for the OH+HBr reaction. The theory also explains well the flat temperature dependence observed for the OH+HCl reaction and the experimentally observed ratio of the rate constants for the OH+HCl and OD+HCl reactions.

Of course, the theory presented here involves several major approximations. In particular, the potential energy surfaces are very approximate and need to be improved by high quality *ab initio* computations. Also, the RBA theory invokes approximations including the neglect of the explicit rotations of the HX molecule and the coupled-states approximation in treating the K quantum number. Furthermore, the spin and orbital angular momenta of the OH radical have not been included in the theory. Despite these approximations, the rovibrational selectivity that is seen in our calculations is so strong that we would expect the basic effects to arise also in more accurate computations and to be seen in experiment.

The two hydrogen atom transfer reactions studied here are both of the heavy–light–heavy type, and the vibrationally selected dynamics follows the pattern expected from quantum studies on atom+diatom reactions using hyperspherical coordinates. Therefore, it is quite probable that the same principles will apply for hydrogen atom transfer reactions involving even larger polyatomic molecules. Furthermore, the calculations presented here provide several new predictions. It is hoped that these predictions might stimulate new experimental work on the state-selected dynamics of the OH+HCl and OH+HBr reactions.

ACKNOWLEDGMENTS

This work was supported by the Science and Engineering Research Council. Support from the Swedish Institute and the EC is also acknowledged.

[1] A. Sinha, M. C. Hsiao, and F. F. Crim, J. Chem. Phys. **92**, 6333 (1990); **94**, 4928 (1991).
[2] M. J. Bronikowski, W. R. Simpson, B. Girard, and R. N. Zare, J. Chem. Phys. **95**, 8647 (1991); M. J. Bronikowski, W. R. Simpson, and R. N. Zare, J. Phys. Chem. **97**, 2194 (1993); **97**, 2204 (1993).
[3] M. J. Frost, P. Sharkey, and I. W. M. Smith, Faraday Discuss. Chem. Soc. **91**, 305 (1991).
[4] G. C. Schatz and H. Elgersma, Chem. Phys. Lett. **73**, 21 (1980); G. C. Schatz, J. Chem. Phys., **74**, 1133 (1981); K. Kudla and G. C. Schatz, *ibid.* **98**, 4644 (1993).
[5] D. C. Clary, J. Chem. Phys. **95**, 7298 (1991).
[6] D. C. Clary, J. Chem. Phys. **96**, 3656 (1992).
[7] D. C. Clary, Chem. Phys. Lett. **192**, 34 (1992).
[8] D. Wang and J. M. Bowman, J. Chem. Phys. **96**, 8906 (1992); J. M. Bowman and D. Wang, *ibid.* **96**, 7852 (1992); D. Wang and J. M. Bowman, *ibid.* **98**, 6235 (1993).
[9] J. Echave and D. C. Clary, J. Chem. Phys. **100**, 402 (1994).
[10] G. Nyman and D. C. Clary, J. Chem. Phys. **99**, 7774 (1993).
[11] D. H. Zhang and J. Z. H. Zhang, J. Chem. Phys. **99**, 5615 (1993).
[12] R. P. Wayne, *Chemistry of the Atmospheres* (Oxford University, Oxford, 1991).
[13] W. B. DeMore, M. J. Molina, S. P. Sander, D. M. Golden, R. F. Hampson, M. J. Kurylo, C. J. Howard, and A. R. Ravishankara, JPL Publication

1987–41, Jet Propulsion Laboratory, California Institute of Technology, Pasadena, CA.
[14] I. R. Sims, I. W. M. Smith, D. C. Clary, P. Bocherel, and B. R. Rowe, J. Chem. Phys. (in press).
[15] P. Sharkey and I. W. M. Smith, J. Chem. Soc. Faraday Trans. **89**, 631 (1993).
[16] J. Römelt, in *The Theory of Chemical Reaction Dynamics*, edited by D. C. Clary (Reidel, Dordrecht, 1986), p. 77.
[17] D. C. Clary, J. Phys. Chem. (in press).
[18] U. Manthe, T. Seideman, and W. H. Miller, J. Chem. Phys. **99**, 10078 (1993).
[19] D. C. Clary and G. C. Schatz, J. Chem. Phys. **99**, 4578 (1993).
[20] K. Kudla and G. C. Schatz, Chem. Phys. **175**, 71 (1993).
[21] G. Nyman and D. C. Clary, J. Chem. Phys. **100**, 3556 (1994).
[22] J. N. Murrell and S. Carter, J. Phys. Chem. **88**, 4887 (1984).
[23] A. R. Ravishankara, P. H. Wine, and J. R. Wells, J. Chem. Phys. **83**, 447 (1985).
[24] D. C. Clary, T. S. Stoecklin, and A. G. Wickham, J. Chem. Soc. Faraday Trans. **89**, 2185 (1993).
[25] D. C. Clary, Annu. Rev. Phys. Chem. **41**, 61 (1990).
[26] A. N. Brooks and D. C. Clary, J. Chem. Phys. **92**, 4178 (1990).
[27] J. C. Light and R. B. Walker, J. Chem. Phys. **65**, 4272 (1976); E. B. Stechel, R. B. Walker, and J. C. Light, *ibid.* **69**, 3518 (1978).
[28] I. Hamilton and J. C. Light, J. Chem. Phys. **84**, 306 (1986).
[29] V. Aquilanti, in *The Theory of Chemical Reaction Dynamics*, edited by D. C. Clary (Reidel, Dordrecht, 1986), p. 383.
[30] A. Ohsaki and H. Nakamura, Phys. Rep. **187**, 1 (1990).
[31] J. M. Bowman and A. F. Wagner, in *The Theory of Chemical Reaction Dynamics*, edited by D. C. Clary (Reidel, Dordrecht, 1986), p. 47; Q. Sun, D. L. Yang, N. S. Wang, J. M. Bowman, and M. C. Lin, J. Chem. Phys. **93**, 4730 (1990).
[32] E. B. Wilson, J. C. Decius, and P. C. Cross, *Molecular Vibrations* (McGraw–Hill, New York, 1955).
[33] A. Persky and M. Broida, J. Chem. Phys. **81**, 4352 (1984).
[34] M. Broida, M. Tamir, and A. Persky, Chem. Phys. **110**, 83 (1986).
[35] G. Herzberg, *Infrared and Raman Spectroscopy of Polyatomic Molecules* (Van Nostrand, New York, 1945).
[36] S. P. Walch and T. H. Dunning, J. Chem. Phys. **72**, 1303 (1980).
[37] M. J. Frisch, M. Head-Gordon, G. W. Trucks, J. B. Foresman, H. B. Schegal, K. Raghavachari, M. Robb, J. S. Binkley, C. Gonzalez, D. J. Defrees, D. J. Fox, R. A. Whiteside, R. Seeger, C. F. Melius, J. Baker, R. L. Martin, L. R. Kahn, J. J. P. Stewart, S. Topiol, and J. A. Pople, Gaussian 90, Revision I, Gaussian Inc., Pittsburgh, PA, 1990.
[38] G. C. Schatz, D. Sokolovski, and J. N. L. Connor, Faraday Discuss. **91**, 17 (1991); Q. Sun, J. M. Bowman, G. C. Schatz, J. R. Sharp, and J. N. L. Connor, J. Chem. Phys., **92**, 1677 (1990)).
[39] A. R. Ravishankara, P. H. Wine, J. R. Wells, and R. L. Thompson, Int. J. Chem. Kinet., **17**, 1281 (1985).
[40] I. W. M. Smith and M. D. Williams, J. Chem. Soc., Faraday Trans. 2 **82**, 1043 (1986).
[41] I. R. Sims, J. Chem. Soc., Faraday Trans. **89**, 2212 (1993).